Dense Optical Flow Applications for Operational Users

Corresponding Author Email:
jason.apke@colostate.edu

Jason Apke[1] , Matthew Rogers[1], Steven Miller[1]
[1]Cooperative Institute for Research in the Atmosphere, Fort Collins, CO

2020 JPSS/GOES-R Proving Ground/Risk Reduction Summit
College Park, MD | P. 24

Introduction

- "Optical Flow" (OF) is the distribution of apparent velocities of movement of brightness patterns in an image (Horn and Schunk 1981)
- ***Deriving OF is a fundamental task in geostationary satellite image analysis***
  1. OF can be used to track features through time sequences
  2. Tracking cloud-drift motion is used to produce operational Atmospheric Motion Vectors (AMVs; Velden et al. 1997; Daniels et al. 2010)
  3. Motion of features can also be used for decision making tools, such as diagnosis of tropical cyclone intensity, derivation of local vertical wind shear, snow vs. cloud identification, or determining observed deep convection severity (Apke et al. 2020)
  4. Using simultaneous scans from a satellite pair, OF serves as a pixel matching method to identify feature altitude (Stereoscopy)
- As satellite imagery improves (in temporal, spatial, spectral, and radiometric resolution), so to does our ability to resolve motion in image pairs
- The goal of this work is to bring cutting edge OF techniques and their benefits to GOES-R series satellite research and operations

Current Optical Flow Techniques

- Most AMV and stereoscopy algorithms use Patch Matching (PM), where targets (e.g. 5x5 pixel boxes) are iteratively compared to candidate targets within a search region in the next image (Fig. 1, Left)
- Tracked features are quality controlled to ensure PM is an efficient and effective OF method
- Quality control removes targets where the sum-of-square-error minimization and cross-correlation maximization to find matching candidates fails
- **Advantages:** Computationally efficient, simple to understand, simple to implement, handles large displacements
- **Disadvantages:** Natural scenes contain motion types which cannot be resolved with PM techniques (Fig. 1, Right), PM only returns motion for a subset of the image pixels (e.g. a Sparse OF system), can be susceptible to noise

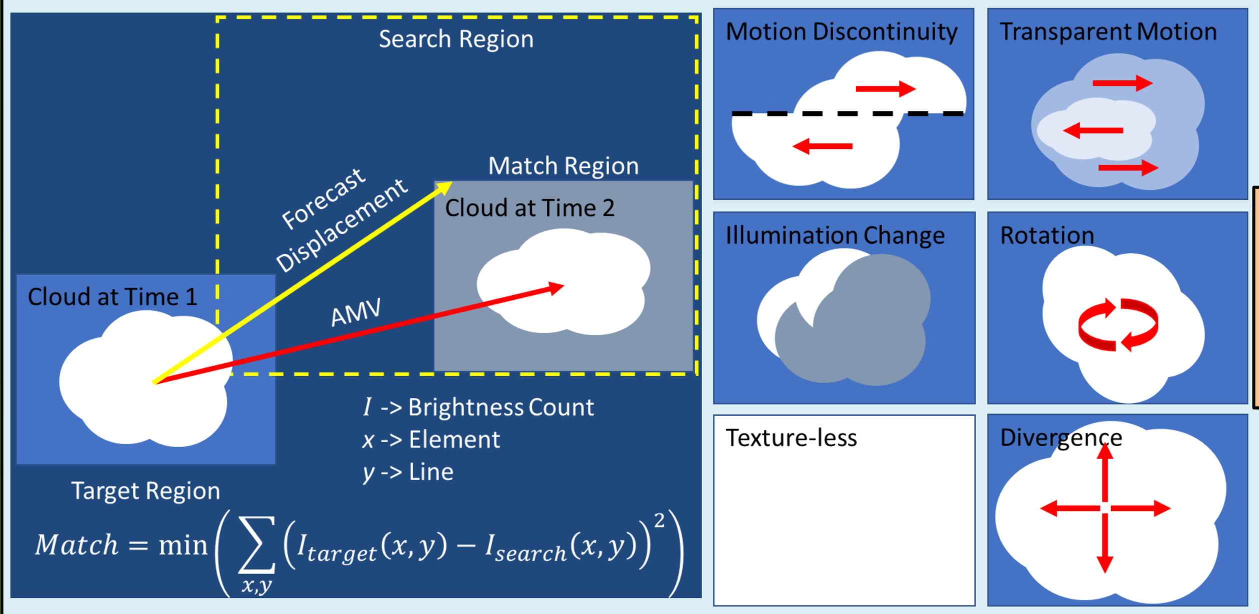

Figure 1. (*Left*) Schematic of the PM Optical Flow scheme, and (*Right*) the types of cloud evolution where PM fails.

Dense Optical Flow Methods

- ***The computer vision community has mitigated or resolved issues associated with the PM techniques to retrieve "Dense" OF fields, where motion is derived at every image pixel (e.g. Fortun et al. 2015)***
- Many DOF derivation methods are based on solving large systems of linear equations set up by assuming a few things about DOF behavior:
  1. The displacements are small
  2. The brightness (or brightness gradient) only changes due to motion
  3. The flow can be regularized (translation or deformation varies slowly)
- ***The temporal resolution of the Advanced Baseline Imager (ABI) improves the assumptions above and enables the derivation of DOF on satellite imagery!***
- At CIRA, we have developed a system of ABI-product leveraging DOF schemes, and are experimenting with applications for satellite remote sensing
- In this poster, we show products that are possible using techniques by Sun et al. (2014) and Farnebäck (2001) to derive DOF modified by ABI channels

Mesoscale Winds

- Combining DOF with cloud-top height products enables AMV-like wind estimation with feature resolution of ~10 km wavelengths (meso-scale)
- Real-time tests show how mesoscale winds can highlight flows relevant to operations (e.g. accelerating horizontal flows with vertical cloud growth Fig. 2)
- Preliminary validation using wind profiling Lidar samples suggest GOES-R DOF derivation approaches are performing on-par with AMVs (Table 1)

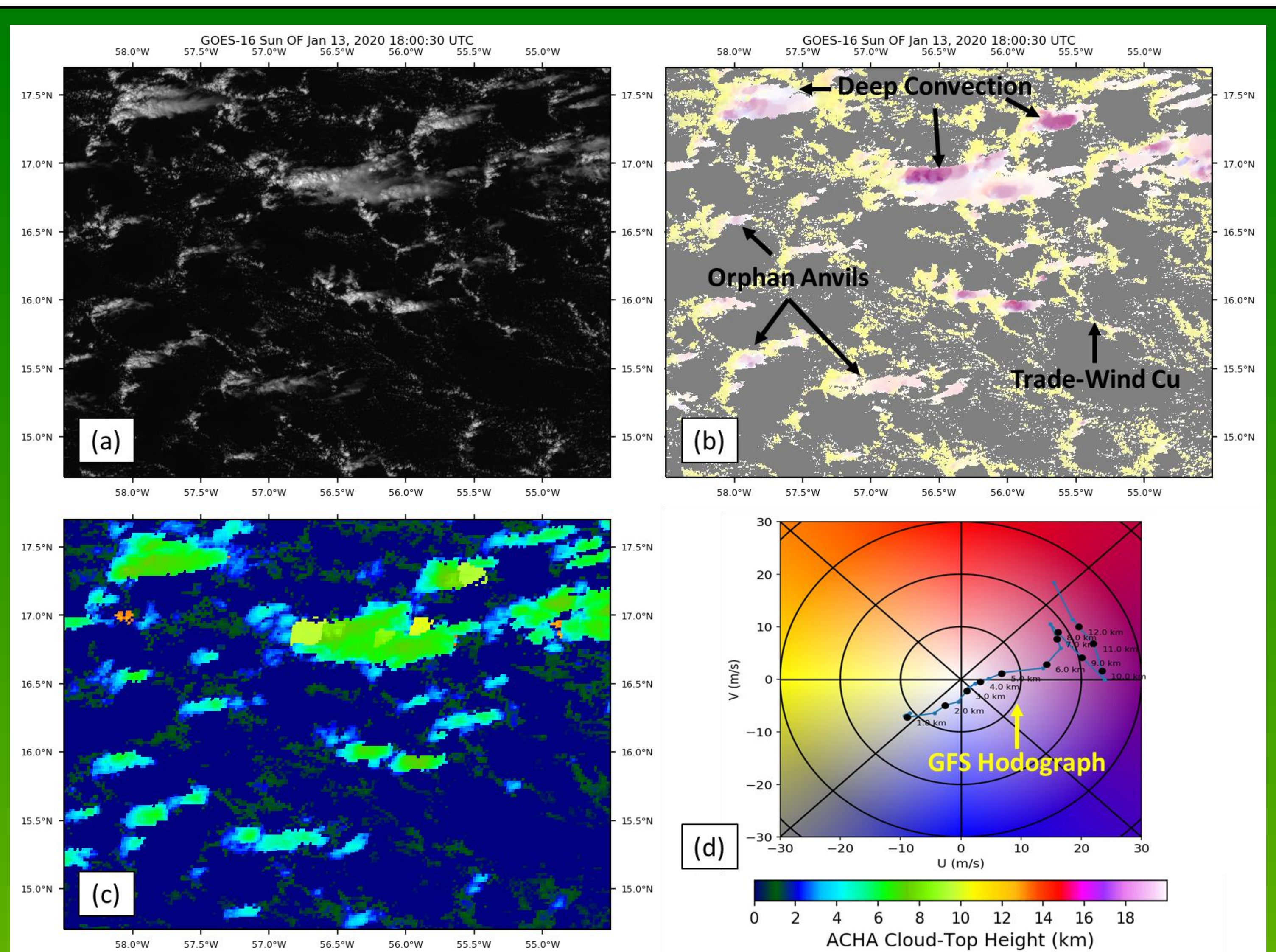

Figure 2. (*Top*) The 13 Jan 2020 GOES-16 a) 0.64-µm visible imagery, b) Sun et al. (2014) dense optical flow (where grey is stationary), c) GOES-R ABI Cloud-Height Algorithm cloud-top heights, and d) color scales used for b) and c), shown with the 18 UTC analysis Global Forecast System vertical wind profile for the region.

Table 1. (*Right*) Validation (Bias/Mean-Vector Difference; MVD) for DOF winds compared to wind-profiling Lidar data, shown with AMV statistics.

Algorithm	Bias (m s^{-1})*	MVD (m s^{-1})*
Modified-Sun et al. (2014) (IR Ch-7)	-0.798	3.101
Farnebäck (2001) (visible imagery)	-0.114	2.272
GOES-R AMVs (IR Ch-7) from Daniels et al. (2018)**	< |-0.5|	~2.9-4.5
GOES-R AMVs (Visible Ch-2) from Daniels et al. (2018)**	< |0.5|	~2.8-3.7

**DOF derived on 23 April 2019 from the GOES-17 meso-sector domain (0055 UTC-0300 UTC) over the pacific coast of the United States, AMV validation statistics come from a larger sample of comparisons to rawinsondes

Figure 3. GOES-16 5-min CONUS Sector CIRA GeoColor product over Hurricane Dorian at a) 1300 UTC and b) 1305 UTC shown with c) the 1302 UTC meso-sector and d) the interpolated GeoColor derived using the Farnebäck (2001) DOF system. Red Arrows highlight the differences between the interpolated product in d) and the actual product in c).

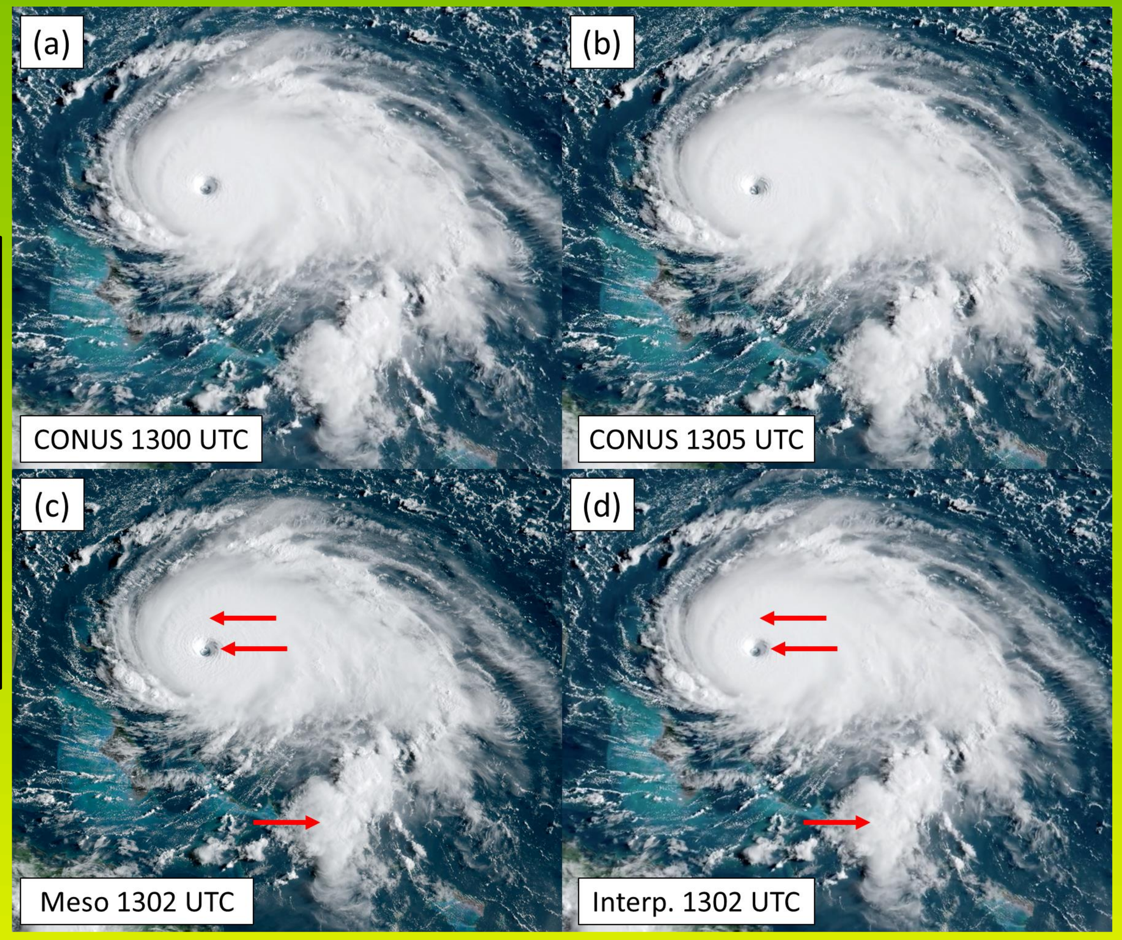

Image Temporal Interpolation

- Brightness motion estimates enable temporal interpolation of products between scanned image frames (e.g. *1-min meso-sectors on demand!*)
- Interpolated GeoColor products highlight important mesoscale motions and are close to true meso-sector imagery (Fig. 3)
- Interpolation struggles in areas with fast motion and deep convection

Image Warping

- Knowing DOF allows research and operational meteorologists to create "warped" images, where brightness (e.g. Fig. 4a) at some previous (or future) time is adjusted in the grid to correct for its motion from the current time
- Without correcting for cloud motion, cloud-top cooling of moving convection sampled in the 10.3-µm infrared band cannot be resolved (Fig. 4b)
- ***Warping is essential*** for operational users and decision-making tools that need time-rates of change for moving fields (e.g. convection initiation cloud-top cooling detected at black arrows in Fig. 4c)

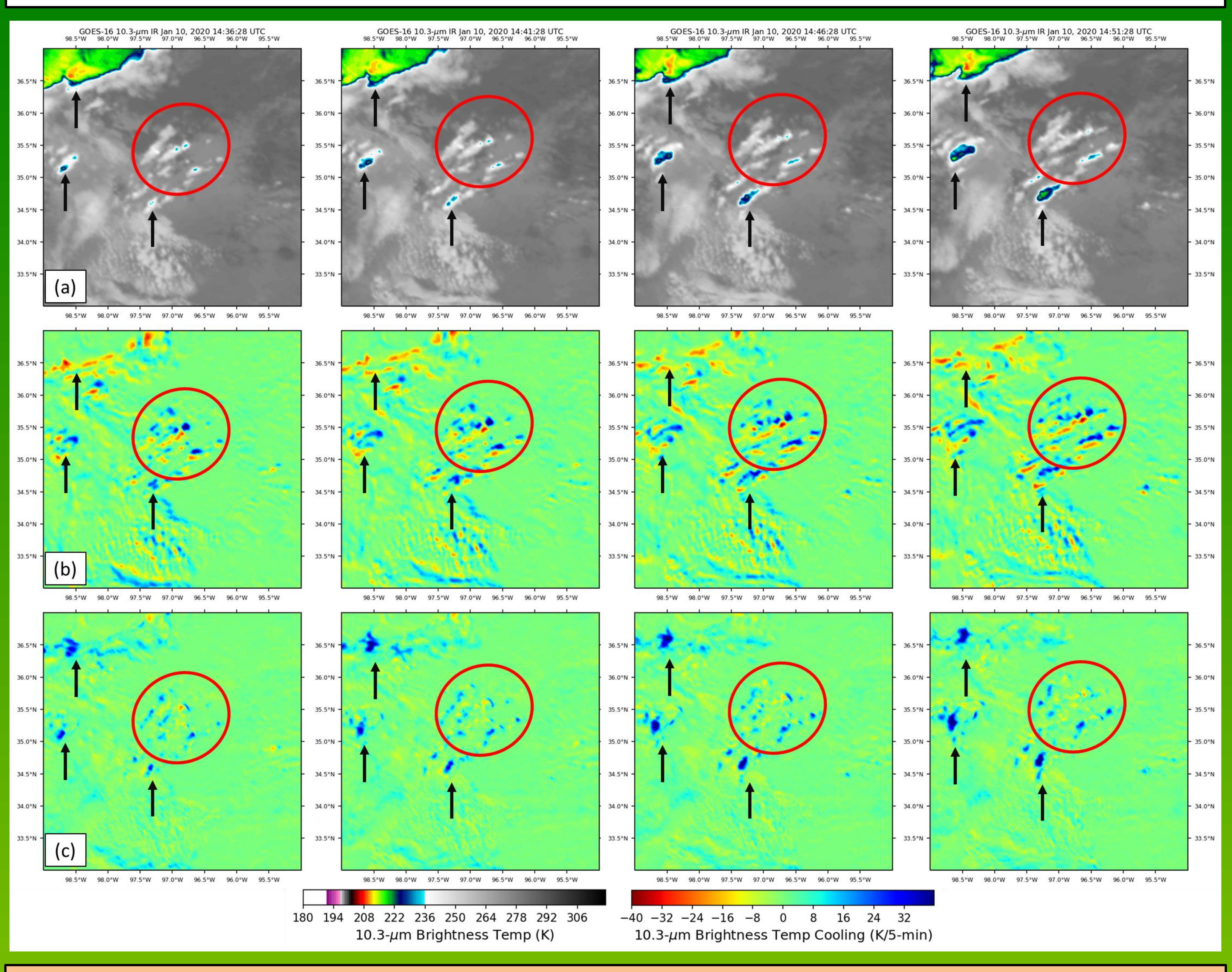

Figure 4. The 10 Jan 2020 GOES-16 column a) 10.3-µm infrared imagery, column b) the 10.3-µm brightness temperature cooling over 5-min without warping for motion, and column c) the 10.3-µm brightness temperature cooling using warping provided by the Farnebäck (2001) DOF algorithm. The black arrows highlight locations of deep convection initiation, and the red circle highlights benign cumulus which produces large cooling magnitudes without correcting for motion.

Other Possible Products

- Several new DOF based products are currently under development, including:
  1. Stereoscopy (cloud-top and feature altitude from multiple satellites)
  2. Feature forward extrapolation
  3. Motion/CIRA product blending
  4. Deep convection cloud-top divergence and vorticity from winds

Conclusions and Future Work

- Successful DOF derivation, now possible with GOES-R series ABI imagery, leads to a myriad of new products for operational and research users
- Winds and interpolation highlight flows important for meteorology operations
- Image Warping enables computation of pixel-level time rates of change for moving fields, such as cloud-top cooling rates of moving convection
- DOF methods are constantly evolving, and research is underway to evaluate cutting edge approaches, and determine how these new approaches will aid in ongoing product development

Acknowledgements: This CIRA team was funded by the GOES-R Program Office, NESDIS GOES-R Program Office award number: NA14OAR4320125. Special thanks to Kristopher Bedka at the NASA Langley Research Center for providing the wind-profiling Lidar data, and to Yoo-Jeong Noh for providing the ACHA cloud-top height data.

Citations

Apke, J. M., K. A. Hilburn, S. D. Miller, and D. A. Peterson, 2020: Towards objective identification and tracking of convective outflow boundaries in next-generation geostationary satellite imagery. *MURI Spec. Ed. Issue Atmos. Meas. Tech.*, Submitted.
Daniels, J. M., W. C. Bresky, S. T. Wanzong, C. S. Velden, and H. Berger, 2010: *GOES-R Advanced Baseline Imager (ABI) Algorithm Theoretical Basis Document for Derived Motion Winds*. 1–60 pp. https://www.goes-r.gov/products/baseline-derived-motion-winds.html.
Daniels, J., W. Bresky, A. Bailey, A. Allegrino, S. Wanzong and C. Velden, 2018: Introducing Atmospheric Motion Vectors Derived from the GOES-16 Advanced-Baseline Imager. *14th Annual Symposium on New Generation Operational Environmental Satellites,* Austin, TX, Amer. Meteor. Soc.
Farnebäck, G., 2001: Two-Frame Motion Estimation Based on Polynomial Expansion. *Proceedings: Eighth IEEE International Conference on Computer Vision*, Vol. 1 of, 171–177.
Fortun, D., P. Bouthemy, C. Kervrann, D. Fortun, P. Bouthemy, and C. Kervrann, 2015: Optical flow modeling and computation : a survey To cite this version : Optical flow modeling and computation : a survey. *Comput. Vis. Image Underst.*, **134**, 1–21. https://hal.inria.fr/hal-01104081/file/CVIU_survey.pdf.
Horn, B. K. P., and B. G. Schunck, 1981: Determining optical flow. *Artif. Intell.*, **17**, 185–203, doi:10.1016/0004-3702(81)90024-2.
Sun, D., S. Roth, and M. J. Black, 2014: A quantitative analysis of current practices in optical flow estimation and the principles behind them. *Int. J. Comput. Vis.*, **106**, 115–137, doi:10.1007/s11263-013-0644-x.
Velden, C. S., C. M. Hayden, S. J. Nieman, W. P. Menzel, S. Wanzong, and J. S. Goerss, 1997: Upper-Tropospheric Winds Derived from Geostationary Satellite Water Vapor Observations. *Bull. Am. Meteorol. Soc.*, **78**, 173–195.